ELSEVIER

PII: S0032-3861(97)00476-X

Polymer Vol. 39 No. 11, pp. 2185–2193, 1998

0032-3861/98/$19.00+0.00

Fourier transform IR study of acid–base interactions: blends of ethylene-vinylacetate copolymer and terpene-phenol resins

M. Brogly*, M. Nardin and J. Schultz
CNRS Institut de Chimie des Surfaces et Interfaces, B.P. 2488, 15 rue J. Starcky, 68057 Mulhouse Cedex, France
(Received 7 October 1996; revised 7 May 1997)

Specific interactions in binary blends of ethylene-vinylacetate copolymer (EVA) with various low molecular weight terpene-phenol tackifying resins (TPR) were systematically investigated, as a function of the composition of the blend and of the electron-acceptor ability of the resin, using attenuated total reflection Fourier transform IR (ATR-FTi.r.) spectroscopy. Molecular acid–base complexes (according to Lewis' electron acceptor–donor concepts) were evidenced between TPR hydroxyl groups and EVA carbonyl groups. Quantitative information on the fraction of acid–base bonded entities, the enthalpy and the equilibrium constant of pair formation were obtained. It appears that the amorphous phases of such polymer blends remain thermodynamically miscible whatever the composition of the blend and the resin acidity. On the contrary, a crystalline transition of the EVA copolymer is observed, depending on the blend composition and resin acidity. This transition is discussed in terms of enthalpy and entropy considerations based on FTi.r. and differential scanning calorimetry (DSC) investigations. Fundamental results are then summarized in order to predict the melting enthalpy of a polymer blend.

(Keywords: acid–base interactions; ATR-FTi.r.; EVA copolymer blends)

INTRODUCTION

Blending of polymers is one of the most studied topics in polymer science in the last five years and appears to be a route to improve specific materials properties. The recent use of polymer blends as bonding and sealing agents[1] (hot-melt adhesives) requires high performance of the blends. In addition to processing abilities these blends have to exhibit high dissipative, cohesive and adhesive properties. Several problems remain unsolved in this area such as the fundamental description of the molecular mechanisms of adhesion. Before focusing our attention on adhesion mechanisms, i.e. on the interfacial specific polymer blend–substrate interactions, the first part of this study is devoted to the analysis of specific electron acceptor–donor interactions in blends of ethylene-vinylacetate (EVA) copolymer and low molecular weight tackifying terpene-phenol resins (TPR), both having complementary chemical structures favouring the establishment of specific interactions by hydrogen bonding. Strong acid–base interactions can greatly favour thermodynamical miscibility even though it is well known that only dispersive forces can lead to miscibility if the solubility parameters are closely matched. Fourier transform IR spectroscopy (FTi.r.) has proved to be a good experimental tool to elucidate both the type and the number of acid–base intermolecular interactions in EVA/TPR blends, as a function of both the composition of the blend and the degree of functionality of the components. Although fundamental bases on the relevance of hydrogen bonding on polymer–polymer miscibility are well stated, for instance in EVA–polyvinylphenol systems[2], one must consider the lack of information (both qualitative and quantitative) concerning the development of the crystalline phase in EVA copolymer even though the amorphous phases remain miscible. This work proposes first to discuss the mechanisms and the magnitude of thermodynamical miscibility in EVA/TPR blends and second to analyse the EVA crystalline phase transition. This transition is obviously related to the magnitude of the thermodynamical miscibility of the amorphous EVA/TPR phase, as will be proved on the basis of FTi.r. and calorimetric measurements.

*To whom correspondence should be addressed. Tel: 33 03 89 60 87 68; Fax: 33 03 89 60 87 99; E-mail: M.Brogly@univ-mulhouse.fr

EXPERIMENTAL DETAILS

Materials

Binary blends of ethylene-vinylacetate copolymer (EVA) with various low molecular weight terpene-phenol tackifying resin (TPR) were studied. The EVA copolymer was supplied by Elf-Atochem (France) and has a vinylacetate content (VA) of 28% by weight. Weight-average and number-average molar masses are respectively 27 000 and 9200 g mol^{-1}. The glass transition temperature T_g and the degree of crystallinity of this EVA are −36°C and 12% respectively, as determined by differential scanning calorimetry (DSC).

Three terpene-phenol resin oligomers TPR1, TPR2 and TPR3 of different degrees of functionality (synthesized by DRT Laboratories (France)) were used. We define d(OH) as the hydroxyl function content of the resin, i.e. the average number of phenol groups per molecule of resin. One molecule can also have 0, 1 or 2 hydroxyl groups (*Figure 1*)

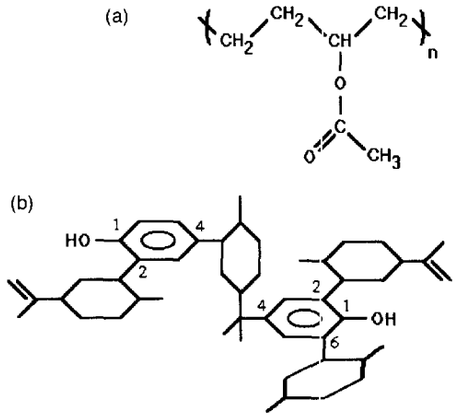

Figure 1 (a) Chemical formula of EVA copolymer. (b) Chemical formula of terpene-phenol resin (d(OH) = 2)

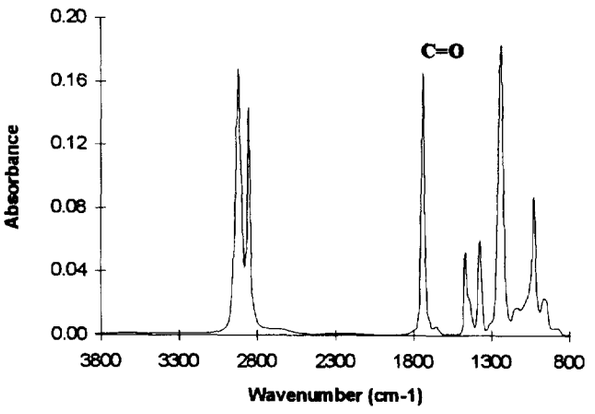

Figure 2 ATR-FTi.r. absorbance spectrum of EVA copolymer

but the average d(OH) values are 0.7, 1.1 and 1.4 phenol groups per molecule for TPR1, TPR2 and TPR3 respectively. One must be aware of the fact that increasing d(OH) is associated with decreasing average molar weight, i.e. number-average molar masses are 600, 520 and 470 g mol^{-1} for TPR1, TPR2 and TPR3 associated with polydispersity indices of 1.40, 1.29 and 1.21 respectively.

Blend compositions of 30:70, 40:60, 50:50, 60:40 and 70:30% by weight of EVA:TPR were prepared by mixing, under inert gas (nitrogen), appropriate amounts of TPR and EVA in a thermally regulated oil bath. Film samples for FTi.r. analysis were obtained by moulding under 1.5 MPa pressure at 150°C.

FTi.r. analysis

IR spectra for polymers and polymer blends were recorded on a Bruker IFS-66 Fourier transform IR (FTi.r.) spectrometer at a resolution of 2 cm^{-1} by averaging 200 scans. Polymer and polymer blend films used in attenuated total reflection (ATR with a KRS5 internal reflection crystal) mode were sufficiently thin to be within an absorbance range (<0.6 absorbance unit) where the Beer–Lambert law is obeyed. In the ATR technique, the IR beam goes through the internal reflection crystal and is reflected at the crystal–sample interface. The evanescent field of the radiation penetrates into the sample and decreases exponentially with distance from the surface. The spectrum is produced in this layer a few micrometres thick. The ATR technique has been shown to be highly sensitive[3] and allows, for a given wavelength λ, an analysis at constant depth, depending on the sample (n_s = 1.5) and internal crystal (n_c = 2.4) refractive indices and on the angle of incidence (θ_i = 45°). ATR spectra show enhanced absorption intensities in the small wavenumber range and reduced intensities at larger wavenumbers. Harrick[4] has defined the penetration depth d_p as the distance required for the electric field amplitude to fall to exp(−1) time of its value at the surface, given by

$$d_p = \frac{\lambda}{2\pi n_c \sqrt{\sin^2\theta_i - (n_s/n_c)^2}} \approx \frac{\lambda}{5}$$

Apart from this distortion absorption effect, bands may be shifted in frequency (2 cm^{-1}) by dispersion effects. As the refractive index of the sample shows dispersion in the wavenumber absorption region, the magnitude of the evanescent electrical field is changed, producing a frequency shift to smaller wavenumbers. This shift simulates a concentration dependence of the wavenumber as it decreases with dilution of the absorbing group in the polymer mixtures. To avoid this error as well as the wavelength dependence of the reflectivity, ATR spectra were systematically corrected and converted into absorbance spectra. This was done using the Bruker proprietary OPUS® software). After correction, quantitative measurements can be performed.

Gaussian and Lorentzian curve fittings of the spectra were obtained using a curve analysis software. The absorption wavenumber, peak width, peak area and peak shape of each individual peak forming the pattern of overlapping bands found in the sample spectrum are then available. In order to appreciate the 'goodness-of-fit' of the band resolution-matching procedure, the root mean square (RMS) derivative was imposed to be less than 0.001, for all the spectra analysed.

Calorimetric analysis

Differential scanning calorimetric (DSC) measurements were performed on a Mettler TA 3000 calorimeter at a 1°C min^{-1} constant heating rate. All the blends were scanned at 200°C min^{-1} from room temperature to 150°C, held for 10 min at 150°C, cooled down to −150°C at 10°C min^{-1}, held 15 min at −150°C and then scanned again to 150°C at 10°C min^{-1}. The glass transition temperatures, heats of fusion and degrees of crystallinity were determined using Mettler TA-72 software. All data are summarized in *Table 3*.

RESULTS

Before studying intermolecular interactions in polymer blends, we briefly report the IR absorption vibrations of the functional groups of pure components, i.e. EVA copolymer and terpene-phenol resins, that may be involved in Lewis electron acceptor–donor interactions. Appropriate FTi.r. techniques must be used depending on the available form of the pure components.

EVA copolymer

Figure 2 presents the ATR absorbance spectrum of EVA copolymer. The absorption band of major interest is the one at 1736 cm^{-1} corresponding to the stretching vibrations of the acetate carbonyl groups, which may exhibit electron donor ability within the blend. According to Lewis' concepts[5,6], the carbonyl group is potentially an electron

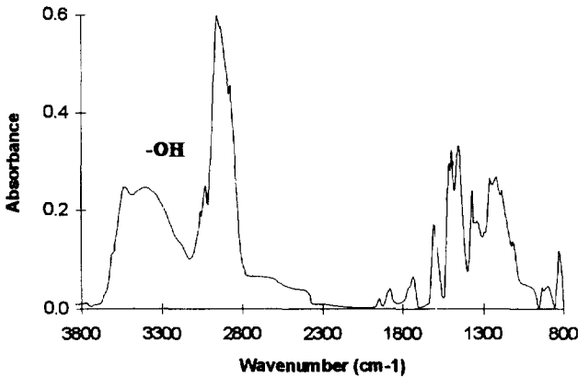

Figure 3 Diffuse-reflectance FTi.r. absorbance spectrum of TPR3

donor group with highest occupied molecular orbital (HOMO) of n type. It can be noted that the acetate functionality is sharply resolved by ATR, the absorption bands at 1236 and 1020 cm^{-1} corresponding respectively to C–O and HC–O stretching vibrations of the acetate.

Terpene-phenol resins

Diffuse reflectance FTi.r. measurements were performed on resins only available as powders. As an example, *Figure 3* presents the spectrum obtained for TPR3. Clear information is given by such a technique after Kubelka Munk treatment, namely[7] four vibration modes (1612, 1585, 1493 and 1465 cm^{-1}) of the aromatic rings, the aromatic rings in-plane (1258 and 1153 cm^{-1}) and out-of-plane (930 and 891 cm^{-1}) C–H vibrations, both depending on the type of phenol substitution (1-2-4 and 1-2-4-6, see *Figure 1*) and, finally, the 3800–3150 cm^{-1} region corresponding to hydroxyl group stretching vibrations.

This last region requires more explanation. *Figure 4* represents the absorption bands of the stretching vibrations of phenol hydroxyl groups for TPR1, TPR2 and TPR3. This peak is rather complex, containing at least three overlapping main bands. By fitting, it is possible to discriminate and calculate the area and absorption wavenumber of these three absorption bands. Prior to the measurements of band areas, the spectra were systematically normalized. Corresponding data are given in *Table 1*. Bands are located respectively at 3610, 3530 and 3430 cm^{-1}. The 3610 cm^{-1} band certainly corresponds[8] to stretching vibrations of the free, or non-hydrogen bonded, phenol hydroxyls. The 3530 and 3430 cm^{-1} bands are attributed[9] to intermolecular associations involving acid–base interactions, namely phenol hydroxyl groups hydrogen bonded between themselves in vicinal oligomers, forming dimers, trimers or multimers. A weak contribution appears near 3200 cm^{-1} and is attributed to the overtone of the fundamentals near 1612 and 1585 cm^{-1}, magnified through Fermi resonance.

However, the two types of phenol substitutions (1-2-4 and 1-2-4-6) induce, owing to steric hindrance, non-equivalent accessibility or electronic distribution of the hydroxyl interacting sites, thus leading to the existence of two absorption bands at higher wavenumbers than for pure polyvinylphenol[10]. A trisubstituted phenol has less electron donor ability than a disubstituted one, because of the non-flatness of the aromatic rings, inducing then, a lower overlapping of the lowest unoccupied (LUMO) and highest occupied (HOMO) molecular orbitals of the acid and the base respectively. As a consequence, the frequency shift observed between free and H-bonded hydroxyl groups is less important in the case of disubstituted–trisubstituted phenol interactions than in the case of stronger disubstituted–disubstituted phenol interactions. These latter are then the most numerous according to *Table 1*. For steric reasons, we suppose that trisubstituted–trisubstituted phenol interactions do not occur. It is of evidence that quantitative results, like the equilibrium constant, cannot be obtained on such bands where self-associated dimers or

Table 1 Hydroxyl group absorption band frequencies and areas for TPR resins

Resin	Band 1		Band 2		Band 3	
	Wavenumber(cm^{-1})	Area(arb. unit)	Wavenumber(cm^{-1})	Area(arb. unit)	Wavenumber(cm^{-1})	Area(arb. unit)
TPR1	3613	2.12	3530	1.50	3430	10.66
TPR2	3610	0.27	3537	4.31	3430	64.36
TPR3	3608	0.35	3537	5.42	3430	95.53

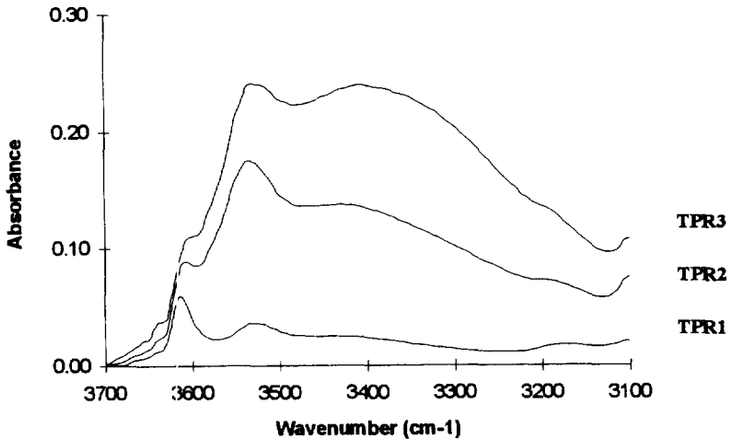

Figure 4 3800–3200 cm^{-1} hydroxyl group absorbance region for TPR1, TPR2 and TPR3

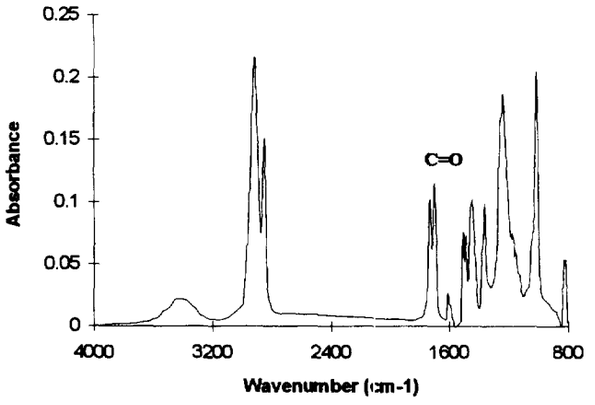

Figure 5 ATR-FTi.r. absorbance spectrum of EVA/TPR3 (50/50) binary blend

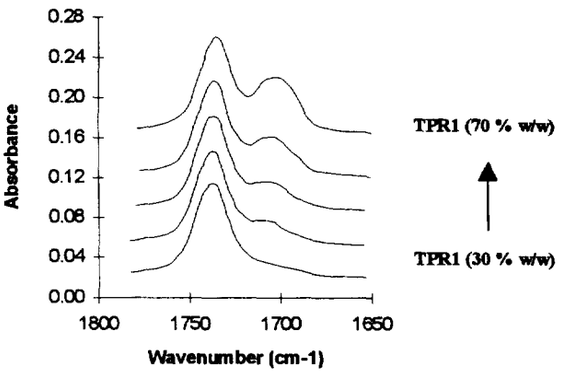

Figure 6 Free and acid–base bonded carbonyl absorption bands as a function of resin content

multimer bands, hydroxyl-ester bands, overtone bands and combination bands are simultaneously present.

Murphy and Rao[11], Pimentel and McClellan[12] and Dean Sherry[13] have published and rewieved a number of enthalpies of hydrogen bond interactions and resulting IR frequency shifts for various systems. One would intuitively expect a relationship between the depth of the curve of potential energy of interaction and the vibrational energy levels involved in frequency shifts. Such a relationship strongly depends on the chemical types of molecules involved in H-bonds. However studies of particular functional groups of molecules give good straight line correlations. A compilation of data for phenols has been proposed by Coleman *et al.*[2]. According to these tabulated data, we propose a linear relationship between the magnitude of the phenol hydroxyl band shifts (in the range 50–200 cm^{-1}) and the acid–base strength of self-association. The order of magnitude of the corresponding enthalpy is -0.083 kJ mol^{-1} per cm^{-1} band shift and the 3610 cm^{-1} band is taken as a reference for free phenol hydroxyls. Self-association frequency shifts are then equal to 80 and 180 cm^{-1} for the 3530 and 3430 cm^{-1} bands, leading to mean values (owing to the dynamic nature of hydrogen bonds) of self-association enthalpies near -7 ± 3 and -15 ± 3 kJ mol^{-1} for trisubstituted and disubstituted phenols involved in Lewis 'n.σ^*' acid–base mechanisms respectively. A hydroxyl group has the ability to act as an electron-donor group through the oxygen HOMO, n, or as an electron-acceptor group through the hydrogen LUMO, σ^*. For pure phenol[9], the enthalpy of self-association reaches -21.8 kJ mol^{-1}, the difference being explained by a deformation due to steric hindrance in the case of TPR.

However, the degree of self-association depends on the absorption coefficient of the hydrogen bonded O–H, which varies considerably with temperature, so that the procedure of measurement of the self-association degree, based on determination of the ratio of free and bonded bands at different temperatures, cannot be used. Furthermore, the intensity of the free band is weak and significantly overlapped by the broad bands due to hydrogen bonded species, so that measurements of peak height or area are subject to large errors, even when applying careful and rigorous curve-resolving procedures. Nevertheless, it is clearly seen (*Table 1*) that the areas of the H-bonded bands increase as the non-H-bonded band decreases, proving that the TPR self-association is unambiguously highly sensitive to the hydroxyl density, d(OH), of the resin.

EVA/TPR blends

Various adhesive formulations were blended, with EVA content ranging from 30% to 70% by weight. The ATR technique, allowing an analysis at a constant depth, of 1.18 μm at 1700 cm^{-1}, performed on 100 μm thick films, reveals (*Figure 5*) first, that the carbonyl stretching band is split in two contributions[14], attributed to the free carbonyl groups (centred around 1736 cm^{-1}) and the acid–base bonded (according to Lewis' electron donor–electron acceptor concepts) carbonyl groups (at 1707 cm^{-1}). This second band is significantly broader than the 1736 cm^{-1} band, which reflects a reasonably wide distribution of hydrogen bond length and geometries in the blend. Secondly, a complex hydroxyl group absorption band is present in the 3800–3150 cm^{-1} region, due to free and H-bonded hydroxyl entities that self-associate (see previous description of phenol self-associations) and inter-associate through acid–base interactions involving EVA carbonyl groups and TPR phenol hydroxyls. Peak locations are 3460 and 3400 cm^{-1}, suggesting a non-equivalence of interacting sites due to the two types of phenol substitution. Further curve-resolving procedures are not conceivable owing to the broadness of the overlapping bands in the 3800–3150 cm^{-1} region. Then, in order to quantify the stoichiometry of acid–base pair formation, curve-fitting is applied to the well resolved absorption region of the carbonyl entities, after correction and conversion of ATR spectra to absorbance spectra. *Figure 6* shows the evolution of the split carbonyl stretching absorption bands as a function of blend ratio for TPR1. The acid–base bonded carbonyl band first appears as a poorly resolved shoulder at low TPR content and, then, becomes highly resolved as the TPR content increases, i.e. as the phenol site density increases.

Quantitative curve-resolving analysis is used to determine the fraction of free and acid–base bonded carbonyl groups as a function of the functionality concentrations in the blend. These quantities can be related to the equilibrium constant that describes the stoichiometry of hydrogen bonding. The additive Beer–Lambert FTi.r. absorption law states that the absorption area A of a functional group is proportional to the optical density, i.e. the molar absorption coefficient ϵ, the concentration of the absorbing species C, and the sample thickness d. The mole number n_i of species i absorbing at the wavenumber ν_i is equal to A_i/ϵ_i and for a

Table 2 Stoichiometric data of acid–base adduct formation for each formulated blend

Resin	EVA (%)	Area AB (C=O)(Abs U *cm^{-1})	Area F (C=O)(Abs U *cm^{-1})	ν shift(cm^{-1})	$f^{AB}_{C=O}$	K^{AB}	D^{AB} (%)
TPR1	30	1.17	1.17	26	0.40	1.58	43
	40	1.29	1.74	25	0.33	1.84	43
	50	1.22	2.44	24	0.25	1.92	37
	60	1.11	3.16	23	0.19	2.51	31
	70	1.09	3.82	22	0.16	5.52	28
TPR2	30	1.37	1.03	26	0.47	0.87	37
	40	1.79	1.40	25	0.46	1.27	47
	50	1.60	2.18	23	0.33	0.95	40
	60	1.52	2.89	23	0.26	1.04	36
	70	1.36	3.64	23	0.20	1.40	31
TPR3	30	1.64	0.86	29	0.56	0.83	36
	40	2.11	1.20	29	0.54	1.08	46
	50	2.58	2.46	29	0.53	1.79	56
	60	2.16	2.46	28	0.37	1.25	46
	70	1.57	3.50	27	0.23	0.81	33

functionality i, the fractions of acid–base bonded (superscript AB) and free (superscript F) groups are given by:

$$f_i^{AB} = 1 - f_i^F = \frac{n_i^{AB}}{n_i^{AB} + n_i^F} = 1 - \frac{n_i^F}{n_i^{AB} + n_i^F} \quad (1)$$

Therefore, we obtain for the carbonyl groups

$$\frac{f^{AB}_{C=O}\epsilon^{AB}_{C=O}}{A^{AB}_{C=O}} = \frac{f^{F}_{C=O}\epsilon^{F}_{C=O}}{A^{F}_{C=O}} = \frac{1}{n^{AB}_{C=O} + n^{F}_{C=O}} = \frac{1}{n^{T}_{C=O}} \quad (2)$$

where $n^T_{C=O}$ is the total number of absorbing carbonyl groups. The fraction of acid–base bonded or free groups is then given by

$$f^{AB}_{C=O} = 1 - f^{F}_{C=O} = \frac{A^{AB}_{C=O}}{A^{AB}_{C=O} + A^{F}_{C=O}\dfrac{\epsilon^{AB}_{C=O}}{\epsilon^{F}_{C=O}}} \quad (3)$$

Assuming that $n^T_{C=O}$, $\epsilon^{AB}_{C=O}/\epsilon^{F}_{C=O}$ and film thickness are not sensitive to a small change in temperature, we can propose for two narrow temperatures:

$$N^{T}_{C=O} = \frac{(A^{AB}_{C=O})_{T1}}{\epsilon^{AB}_{C=O}} + \frac{(A^{F}_{C=O})_{T1}}{\epsilon^{F}_{C=O}} = \frac{(A^{AB}_{C=O})_{T2}}{\epsilon^{AB}_{C=O}} + \frac{(A^{F}_{C=O})_{T2}}{\epsilon^{F}_{C=O}} \quad (4)$$

leading to

$$\frac{\epsilon^{AB}_{C=O}}{\epsilon^{F}_{C=O}} = \frac{(A^{AB}_{C=O})_{T2} - (A^{AB}_{C=O})_{T1}}{(A^{F}_{C=O})_{T1} - (A^{F}_{C=O})_{T2}} \quad (5)$$

Practically, for polyvinylphenol–EVA blends, the ratio of molar absorption coefficients (equation (5)) was found[15,16] equal to 1.5 ± 0.1 for spectra recorded between room temperature and 90°C. This value was determined in the literature on the basis of transmission experiments. That is why all the spectra we have recorded by ATR were systematically converted to absorption-like spectra. Curve-fitting performed on each spectrum shows that the band shapes are mixed between Gaussian band type (ranging from 91% to 96%) and Lorentzian band types (ranging from 4% to 9%). Although the value of 1.5, taken from the literature, was determined on the basis of pure Gaussian band shapes, we consider that the high fraction of Gaussian band in our mixed shapes renders the 1.5 value valid for our homostructural TPR–EVA systems. Absorption area, frequency shifts, and fraction of free and acid–base bonded carbonyls are gathered in *Table 2*, for each formulated blend. Moreover, we are able to calculate the apparent equilibrium constant of the acid–base reaction. Assuming that the acid–base reaction leads to the formation of a 1:1 complex [–OH] + [–C=O] ⇔ [–OH- - -O=C–], and defining [–OH] and [–C=O] as the respective molar concentrations of carbonyl and hydroxyl groups available in the blend, then the apparent equilibrium constant is given by

$$K^{AB} = \frac{f^{AB}_{C=O}}{F^{F}_{C=O}([OH] - f^{AB}_{C=O}[C=O])} \quad (6)$$

Knowledge of the vinylacetate content (28% by weight, 11.2% by mol) of the EVA copolymer allows us to calculate the molar concentration of carbonyl groups per weight unit of EVA, i.e. [C=O] = 3.25 mol/w.u. We also propose for TPR2 and TPR3, on the bases of number-average molar masses and, to a first approximation in consideration of their low polydispersity indices, a phenol concentration by weight unit of resin, [O–H] = $(1000/M_n)d$(OH), of 1.16, 2.11 and 2.98 mol/w.u. for TPR1, TPR2 and TPR3 respectively. Values of the apparent equilibrium constants are gathered in *Table 2*. Moreover, considering the mole number of functional C=O and OH entities present in a given blend we are able to express the degree of acid–base inter-associations between phenol and carbonyl groups D^{AB} as

$$D^{AB} = \frac{2f^{AB}_{C=O}[C=O]}{f^{EVA}_{Blend}[C=O] + f^{TPR}_{Blend}[O-H]} \quad (7)$$

where f^{EVA}_{Blend} and f^{TPR}_{Blend} are the weight fractions of EVA and TPR in the blend. Corresponding data are reported in last column of *Table 2*. *Figure 7*(a–c) show the evolution of $f^{AB}_{C=O}$, D^{AB}, and K^{AB} with both the EVA content of the blend and the Lewis acidity of the resin.

DISCUSSION

As shown in *Figure 7*(a), for the three formulated series, the fraction of acid–base bonded carbonyls increases as the terpene-phenol content of the blend increases. In other words, on the basis of simple entropic considerations, the probability that a single carbonyl group will form an n.σ^* adduct with a phenol group increases as the phenol content increases. Such results are fully consistent with literature results[17]. *Figure 7*(a) reveals also that $f^{AB}_{C=O}$ increases as the functionality degree of the resin does. This is common for hydrogen bonded systems where one of the components self-associates: as a result more acid–base bonds between unlike molecules can be formed upon mixing than those formed between like molecules, leading to a gain in entropy.

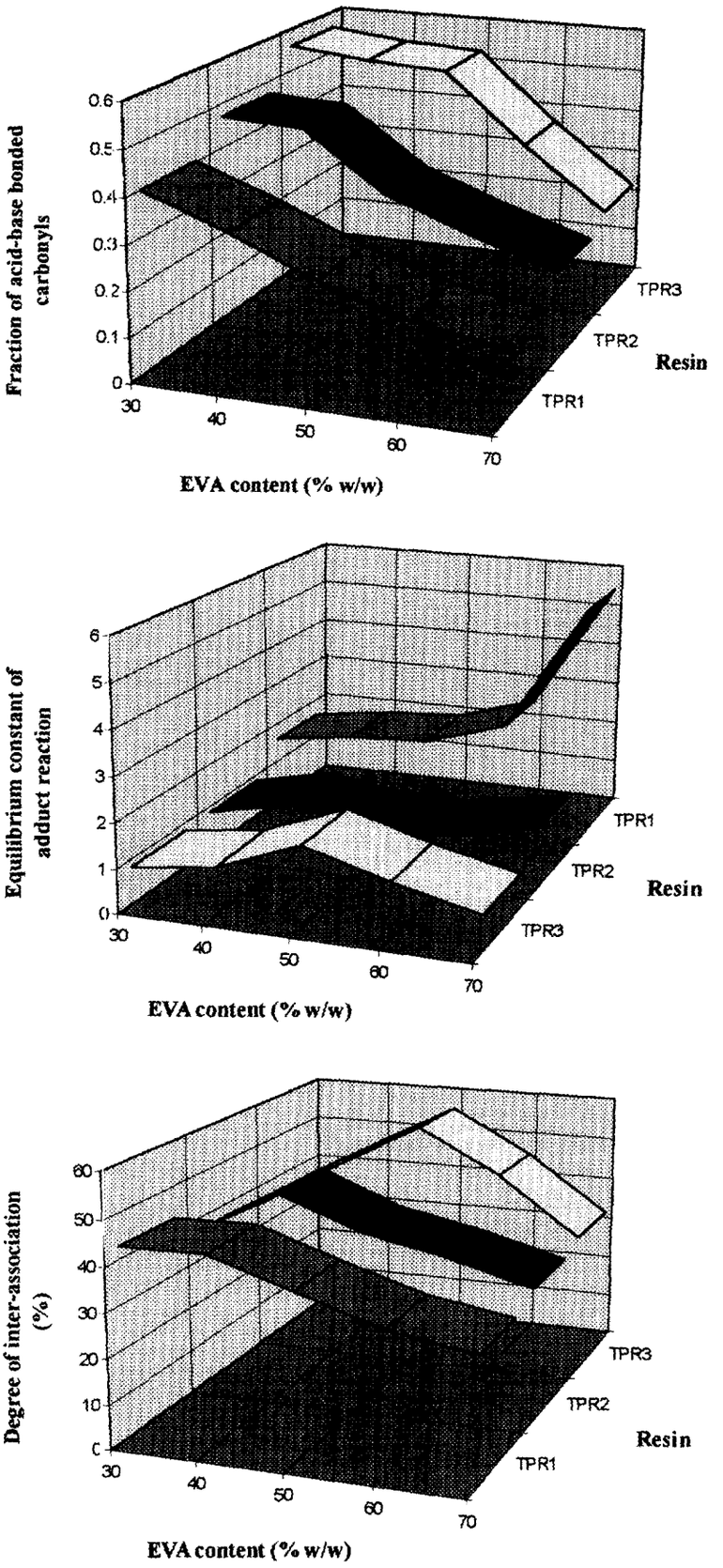

Figure 7 (a) Evolution of $f_{C=O}^{AB}$ with EVA content and functionality degree of the resin. (b) Evolution of the equilibrium constant of adduct reaction as a function of EVA content and functionality degree of the resin. (c) Evolution of the degree of adduct inter-association as a function of EVA content and functionality degree of the resin

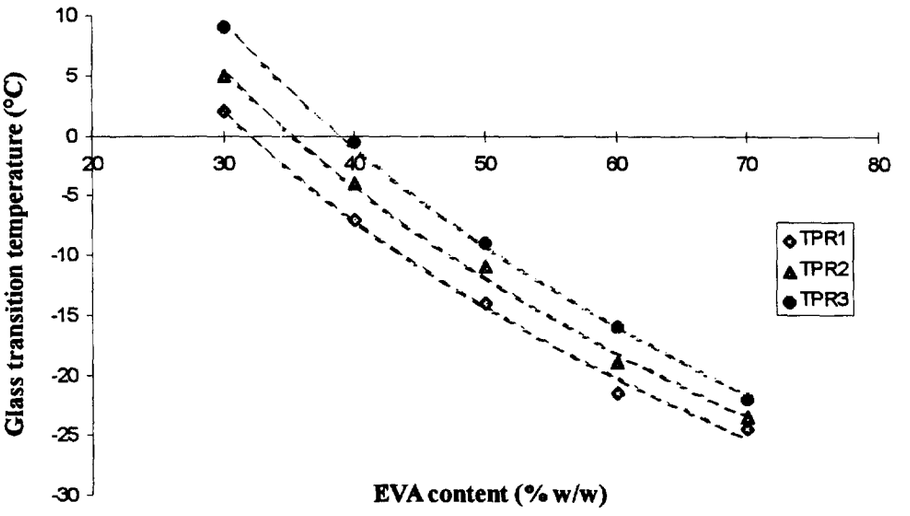

Figure 8 Evolution of the glass transition temperature as a function of EVA content and functionality degree of the resin

These effects favour a higher value of the free energy of mixing. As observed, the maximum $f_{C=O}^{AB}$ values obtained, for the three formulated series, range from 0.40 to 0.56. Such results were observed in the case of polymer–solvent interactions[15,16]. Moreover, this study clearly points out the major effects of the resin functionality degree on $f_{C=O}^{AB}$. *Figure 7*(b) reveals, for blends containing TPR1, a constant increase of the apparent equilibrium constant with the EVA content. This result seems consistent with classical[18] evolution of K^{AB}. For blends involving TPR2 and TPR3 with various amounts of EVA, *Figure 7*(b) shows, first, the existence of a maximum of the equilibrium constant of the acid–base reaction and, secondly, the shift of this maximum to lower TPR content, when d(OH) is increased. These results appear surprising compared to previous published results[2], where the equilibrium constant was found to increase with the amount of EVA (with VA content equal to 70 or 45 wt.%, i.e. amorphous copolymers). The physical meaning of K^{AB} is the efficiency of the stoichiometric reaction of adduct association. As d(OH) increases, the fraction of trisubstituted phenols increases, relative to disubstituted ones. Therefore, for d(OH) values greater than unity, even with low TPR content, a fraction of trisubstituted phenols remains unbonded for steric reasons, leading to a decrease of K^{AB}, contrary to disubtituted phenols of TPR1 (d(OH) = 0.7) which will certainly interact with carbonyl.

Figure 7(c) shows a maximum in the dependence of D^{AB}, which represents the fraction of functional groups involved in acid–base mechanisms with respect to the total number of functionalities ([OH] and [C=O]) present in the blend, on the EVA content and d(OH). This maximum indicates that, for a given blend nature and ratio, the number of acid–base pairs formed is maximum. Then, if the blend ratio increases, even a little, i.e. when the fraction of EVA copolymer in the blend increases relative to the terpene-phenol fraction, then the number of EVA carbonyl groups present is in excess relative to the number of TPR hydroxyls. Potentially, all the hydroxyls which have the ability to adduct would succeed in doing so, but, according to a 1:1 stoichiometric law, a fraction of the EVA carbonyls would be left unbonded, leading to a decrease of both K^{AB} and D^{AB}.

At this stage, two questions should be asked: do the amorphous phases of the blends remain miscible and how is this maximum related to the semi-crystalline nature of our EVA (28 wt.% VA) copolymer?

The glass transition temperatures T_g of all the blends are collected in *Figure 8*. The T_g value is unique, for all blends, whatever d(OH) and the EVA:TPR ratio. The amorphous phases of all samples are then miscible. Several theoretical equations have been proposed to explain the T_g versus composition behaviour of miscible binary polymer mixtures, depending on the strength[19] of interaction between components or on the fraction of flexible branches[20] in the polymers involved. We decided to fit experimental data with a free volume additive model[21]. To a first approximation, assuming that the coefficient of free volume expansion α is equal for two polymers A and B in the melted state, we express the T_g of the blend as

$$T_{gm} = \phi_A T_{gA} + \phi_B T_{gB} + \frac{k_c}{\alpha}\phi_A \phi_B \qquad (8)$$

where ϕ_A and ϕ_B are the volume fractions of A and B type polymers. k_c is defined as a free volume coupling factor of amorphous phases A and B. Dotted lines on *Figure 8* represent the fitted T_g versus composition curves, which are in good agreement with the experimental results. k_c values obtained are respectively −0.038, −0.025 and −0.021 for TPR1, TPR2 and TPR3 respectively. Negative values correspond to a free volume increase due to blending. Therefore, at a given blend ratio, T_g i.e. the segmental mobility of the amorphous phase, decreases with d(OH). This effect can be attributed to an increase of the strength of acid–base interactions or of D^{AB} with d(OH). In order to estimate the strength of interaction, two methods are proposed. The first consists in plotting the equilibrium constant of the adduct reaction versus reciprocal temperature. The interest in working at high temperature consists in studying liquid–liquid phase separation. Many results are available in the literature[2], but the aim of the present study is not to study high temperature miscibility. The second method, proposed by Fowkes[22], states that the stretching frequency of an acid–base bonded carbonyl oxygen is decreased by an amount $\Delta\nu^{AB}$, proportional to the enthalpy of bonding ΔH^{AB}. By comparison of the enthalpies of acid–base complexation, between ethylacetate and Lewis acids of various types and strengths, determined by microcalorimetry and FTi.r. frequency shifts, Fowkes proposed the following linear

Table 3 Calorimetric data of EVA/TPR formulated blends

Resin	EVA (%)	T_g(°C)	ΔH_f(J g^{-1})	Crystallinity(%)
TPR1	30	2	1	0.3
	40	−7	2.5	0.9
	50	−14	3.9	1.3
	60	−21.5	7.5	2.6
	70	−24.5	12.3	4.2
TPR2	30	5	0	0
	40	−4	0.3	0.1
	50	−11	2.6	0.9
	60	−19	5.5	1.9
	70	−23.5	10	3.4
TPR3	30	9	0	0
	40	−0.5	0	0
	50	−9	0	0
	60	−16	2.8	1
	70	−22	7	2.4

correlation (coef. 0.999) between ΔH^{AB} and $\Delta\nu^{AB}$:

$$\Delta H^{AB}_{C=O} = -0.99\Delta\nu^{AB}_{C=O} \quad (9)$$

Frequency shifts given in *Table 2*, allow us to propose average values of enthalpies of acid–base interactions of 24, 27 and 28 kJ mol^{-1} for TPR1, TPR2 and TPR3 respectively. These results are in good agreement with literature data (−21.3 kJ mol^{-1} for EVA/PVPh blends[15,16] and −23.8 kJ mol^{-1} for ethylacetate/phenol blends[23]), and also reveal that interaction strengths, within error, do not change significantly with increasing hydroxyl density.

We can now focus on the semi-crystalline nature of the EVA copolymer. The decrease of the degree of inter-association was previously attributed to an excess of carbonyl functionalities relative to hydroxyl groups, and, although the amorphous EVA/TPR phase remains miscible, a fraction of EVA carbonyl groups were left unbonded. Thermodynamical considerations evidence the balance between the decrease of the free enthalpy of mixing (through specific acid–base interactions) due to an excess of EVA and the increase of the enthalpy of crystallization. Experimental melting enthalpies gathered in *Table 3* clearly evidence that the development of a crystalline EVA phase (not involved in acid–base n.σ^* mechanisms) in the blend is related to the decrease of the degree of inter-association D^{AB} of the amorphous phase. The maximum value of D^{AB} can be defined as a crystalline threshold (CT). Then, assuming first the formation of 1:1 adduct between carbonyls and hydroxyls and secondly that the remaining fraction of unbonded EVA may crystallize, we are able to estimate, for each blend, the value of the enthalpy of fusion as

$$\Delta H_f^{Blend} = \frac{f^{EVA}_{Blend}[C=O] - f^{TPR}_{Blend}[O-H]}{[C=O]}\Delta H_f^{EVA} \quad (10)$$

where ΔH_f^{EVA} is the enthalpy of fusion of pure EVA. Calculated and experimental values ΔH_f^{Blend} are reported, versus EVA content, in *Figure 9*. This figure shows similar evolution between calculated and experimental data. The hypothesis that the maximum value of the degree of inter-association corresponds to a crystalline threshold is evidenced and moreover proves that carbonyl groups trapped in the crystalline phase do not contribute, in terms of frequency shift, to the acid–base bonded carbonyl band. This threshold increases with the hydroxyl density of the resin, i.e. the dilution of EVA macromolecular chains in TPR molecules increases with d(OH), leading to higher values of the free enthalpy of mixing.

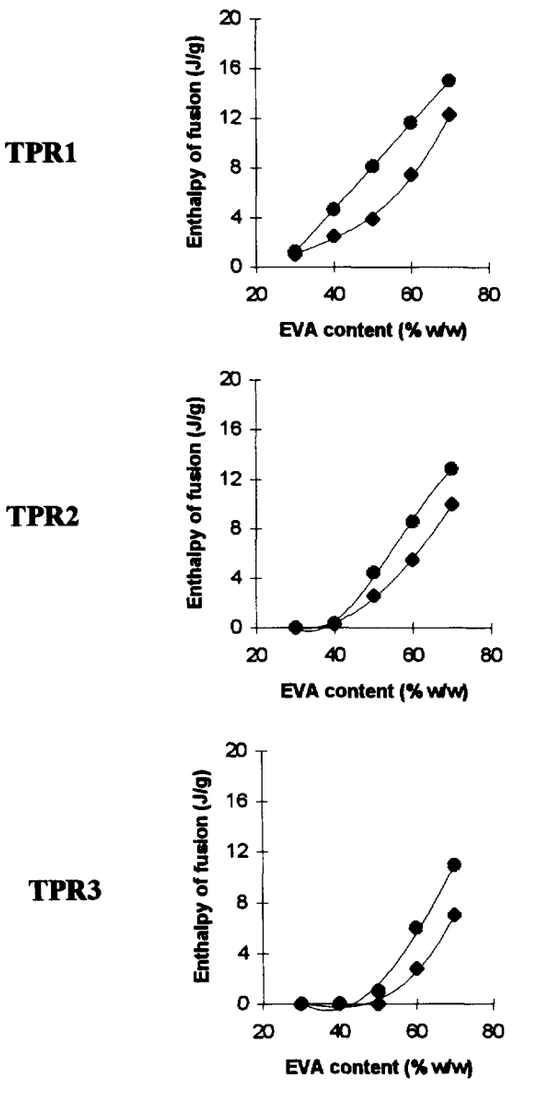

Figure 9 Evolution of the enthalpy of fusion as a function of EVA content and functionality degree of the resin (● calculated and ♦ experimental data)

CONCLUSION

In the present study, using ATR-FTi.r. spectroscopy, acid–base self-associations (n.σ* according to Lewis' concepts) in blends of EVA and terpene-phenol resins are evidenced between carbonyl and phenol hydroxyl groups. Quantitative curve-resolving analysis allows us to determine the fraction of carbonyl groups linked through acid–base interactions as well as the degree of inter-association in the blends, on the basis of 1:1 adduct formation. Therefore, we demonstrate that low VA content EVA copolymer (28 wt.%) can exhibit a high fraction of acid–base n.σ* adducts when blended with a strong Lewis acid component. Moreover, this study clearly points out the major effects of the functionality degree of the resin on the amount of acid–base bonded species. Calorimetric measurements show the thermodynamic miscibility of the amorphous phase for all the blends. A free volume additive model is applied to explain the T_g versus composition behaviour of the miscible binary polymer mixtures. It is shown that the segmental mobility of the amorphous phase decreases with d(OH) at a given EVA:TPR blend ratio. Finally, the evolution of the degree of self-association is related to the semi-crystalline nature of the EVA copolymer. The decrease, at high EVA content, of the degree of inter-association is proved (through experimental and calculated data) to be due to crystallization of EVA macromolecular chains. The maximum value of D^{AB} is defined as a crystalline threshold. This threshold is shown to depend on the balance between carboryl and phenol hydroxyl functionalities through both d(OH) and blend ratio, i.e. on the ability of TPR acid molecules to dilute EVA macromolecular chains.

REFERENCES

1. Gauthier, M. M. in Adhesives and Sealants, Engineered Materials Handbook, ASM International, New York, 1990.
2. Coleman, M. M., Graf, F., Painter, P. C. in Specific Interactions and the Miscibility of Polymer Blends, Technomic Publishing, Basel, 1991, p. 257.
3. Braun, D., Böhringer, B. and Eidam, N., *Polym. Bull.*, 1989, **21**, 63.
4. Harrick, N. J. in Internal Reflection Spectroscopy, Harrick Scientific Co., New York, 1987.
5. Lewis, G. N. in Valence and the Structure of Atoms and Molecules, Chemical Catalog Co., New York, 1923.
6. Jensen, W. B. in The Lewis Acid–Base Concepts, Wiley, New York, 1979.
7. Hummel, D. O. in Infrared Analysis of Polymer Resins and Additives: an Atlas, Wiley-Interscience, New York, 1971.
8. Bellamy, L. J. in The Infrared Spectra of Complex Molecules, 3rd edn., Chapman and Hall, London, 1975.
9. Whetzel, K. B., Lady, J. H. in Spectrometry in Fuels, Friede, Plenum, London, 1979, p. 259.
10. Lee, J. Y., Moskala, E. J., Painter, P. C. and Coleman, M. M., *Appl. Spectrosc.*, 1986, **7**, 991.
11. Murphy, A. S. M. and Rao, C. N. R., *Appl. Spectrosc. Rev.*, 1968, **2**, 69.
12. Pimentel, G. C. and McClellan, A. L., *Ann. Rev. Phys. Chem.*, 1971, **22**, 3247.
13. Dean Sherry, A. (Eds. P. Schuster, G. Zundel, and C. Sandorfy), The Hydrogen Bond, Vol. III, North-Holland, Amsterdam, 1976.
14. Moskala, E. J., Runt, J. P., Coleman, M. M., in Multicomponents Polymer Materials, Advances in Chemistry, Series 211, Paul and Sperling, ACS, Washington DC, 1986.
15. Moskala, E. J., Howe, S. E., Painter, P. C. and Coleman, M. M., *Macromolecules*, 1984, **17**, 1671.
16. Coleman, M. M., Xu, Y. and Painter, P. C., *Macromolecules*, 1994, **27**, 127.
17. Coleman, M. M., Lichkus, A. M. and Painter, P. C., *Macromolecules*, 1989, **22**, 586.
18. Painter, P. C., Park, Y. and Coleman, M. M., *Macromolecules*, 1989, **22**, 570.
19. Couchman, P. R., *Macromolecules*, 1987, **20**, 1712.
20. Di Marzio, E. A., *Polymer*, 1990, **31**, 2294.
21. Marin, G., Menezes, E., Raju, V. R. and Graessley, W. W., *Rheol. Acta*, 1980, **19**, 462.
22. Fowkes, F. M., Tischler, D. O., Wolfe, J. A., Lannigan, L. A., Ademu-John, C. M. and Halliwell, M. J., *J. Polym. Sci., Polym. Chem. Ed.*, 1984, **22**, 547.
23. Pimentel, G. C., McClellan, A. L. in The hydrogen bond, W. H. Freeman, San Francisco, CA, 1960.